Journal of Structural Geology, Vol. 6, No. 4, pp. 433 to 437, 1984
Printed in Great Britain

0191-8141/84 $03.00+0.00

Strain analysis of passive elliptical markers: success of de-straining methods

GRAHAM JOHN BORRADAILE

Department of Geology, Lakehead University,
Thunder Bay, Ontario P7B 5E1 Canada

(*Received* 5 *January* 1983; *accepted in revised form* 31 *October* 1983)

Abstract—Where passive elliptical markers are homogeneously and coaxially strained the strain ellipse ratio may be estimated to within 10%. This takes account of inaccuracies in measurement and does not assume knowledge of the strain ellipse's orientation. Between 50 and 75 markers are needed to achieve this accuracy and larger sample sizes do not significantly improve on this. The de-straining methods use two different tests for randomness of the de-strained fabric. One of these, the runs test, is particularly sensitive to clustering in the angular distribution and may be of particular value in de-straining sedimentary fabrics. De-straining methods are warranted where the strain ellipse ratio is ≥3.0 in natural data.

INTRODUCTION

CONSIDERABLE attention has been paid to the analysis of strain of homogeneously and passively deformed elliptical markers (Ramsay 1967, Dunnet 1969, Dunnet & Siddans 1971, Harvey & Ferguson 1981, Lisle 1977a, 1977b, Matthews *et al.* 1974, de Paor 1980, Seymour & Boulter 1979, Shimamoto & Ikeda 1976, Siddans 1980a, b, Le Theoff 1979, Peach & Lisle 1979). The hope is that naturally occurring objects which may be approximately ellipsoidal can, under some circumstances, behave passively and that the various refinements of Ramsay's 'Rf/ϕ' approach may be applied. In practice, successful and easy applications of the Rf/ϕ approach are most likely to occur where homogeneous strains have accumulated coaxially and where both the angular-distribution and the shape-distribution of the markers was random prior to strain. These ideal conditions form premises for the tests in this paper.

In this article I attempt to illustrate the accuracy and precision of two methods of applying the Rf/ϕ de-straining approach, taking into account the nature of the initial angular distribution of the markers' long axes, the propagation of observational errors on the markers' shapes and orientations, the range of shapes of the original markers and the sample-size. Throughout, note has been taken of the circular nature of the widely dispersed angular-distributions (Mardia 1972).

Where null hypotheses have been tested statistically a significance level of $\alpha = 0.05$ has been chosen; we are willing to take a 1 in 20 chance that we will reject a hypothesis when it is actually true. Samples in the range 50–200 are considered large, less than 50 are considered to be small.

To avoid confusion, a group (an array) of elliptical markers which has not yet been deformed will be termed a pre-strain array. After deformation this is termed a strained array. If some algebraic processes are applied to restore the strained array to its original pre-strain condition it will be termed a de-strained array. This avoids the ambiguity of the commonly used term 'undeformed' which could imply that an object or array never was strained or alternatively that it has had its state of strain algebraically removed.

The theme of the work described here is to follow Siddans (1980a, b) and model pre-strain arrays of elliptical markers and then strain them by known amounts to simulate strained arrays of elliptical markers. This simulated field data on strained markers has then been analysed by the minimisation methods to determine the success of the strain analysis methods and other tests associated with them. Since the strains are actually known it is possible to determine the effectiveness of the methods under different conditions. The computer programs used were different from that used by Peach & Lisle (1979).

The fundamental equations relating the initial shape axial ratio ($\sqrt{R_o}$), finite-strain ellipse ratio ($\sqrt{R_s}$) marker shape-ratio ($\sqrt{R_f}$), initial orientation (θ) and final orientation (ϕ) with respect to the principal extension directions are for a single elliptical marker:

$$\tan 2\phi = \frac{2R_s^{\frac{1}{2}}(R_o - 1)\sin 2\theta}{(R_o+1)(R_s-1)+(R_o-1)(R_s+1)\cos 2\theta} \quad \text{(Ramsay eqn. 5-22)}$$

$$R_f = \frac{\tan^2\phi(1 + R_o\tan^2\theta) - R_s(\tan^2\theta + R_o)}{R_s\tan^2\phi(\tan^2\theta + R_o) - (1 + R_o\tan^2\theta)}. \quad \text{(Ramsay eqn. 5-27)}$$

These formulae, or variants of them, are used for transforming the individual elliptical markers' axial ratios and long-axis orientations in either straining or de-straining processes. In the simpler case of rigid markers, Borradaile (1976) applied a χ^2-minimum method to optimise the goodness-of-fit of a de-strained array and a model of it. Lisle (1977a) has extended this to passive elliptical markers. In his method the arrays of strained markers are de-strained in successive steps, using a different de-straining ratio each time. (In this study the optimum incremental change in the de-straining ellipse axial ratio was found to be 0.01). The reciprocal strain ellipse is applied in a direction which is believed to be

perpendicular to the strain ellipse (Dunnet & Siddans 1971, p. 316). The intention is that at some step in the process we will choose a de-straining ratio which successfully restores the array of markers to its pre-strain state. Our attention should be focused on three items:

(1) the orientation of the strain ellipse is unknown;
(2) the original orientation-distribution of the markers is unknown (if it is believed to be random this can be modelled) and
(3) a method for comparing the de-strained array with the modelled pre-strain array must be selected.

Assuming that these matters can be resolved the de-strained array is compared with its modelled pre-strain equivalent until the best-fit is found (given by a minimum value of a statistic). At this point the de-straining ellipse should have the same axial ratio as the strain ellipse which produced the observed deformation.

Simulation of observations of tectonically strained markers

Arrays of pre-strain elliptical markers were created. The angular distributions were selected randomly over the complete angular range. The axial ratios of the markers' shapes were also selected randomly over the range 1.0–2.25. (A weak unimodal shape distribution produces little difference). In the main batch of tests illustrated, sample sizes were 25, 30, 40, 50, 75, 100 and 200 markers. A total of 108 different arrays were generated to provide a meaningful test of the de-straining methods at each sample size.

Each pre-strain array was then strained by known amounts in known directions to simulate data on naturally deformed, homogeneously and coaxially strained passive markers. Ten finite strain ratios were used: $\sqrt{R_s}$ = 1.1, 1.2, 1.3, 1.41, 1.5, 1.73, 2.0, 3.0, 4.0 and 5.0. Thus 1080 different simulations of field data on tectonically strained markers were available for testing.

Simulation of observational errors

Hitherto, the strain analysis methods of the Rf/ϕ family have been applied on the assumption that the observed data on naturally occurring elliptical strain markers are measured with sufficient accuracy that this need not be taken into consideration in determining the strain. The present simulations defined initial ellipse axial ratios and orientations with at least eight significant figures, and the simulated strained array similarly had angles and axial ratios specified with an unrealistic precision and accuracy! How much would the results of our strain analyses be affected if we had to measure the angles with a protractor and measure the markers' axial lengths with a rule in the field?

I studied such effects using ellipses draughted with engineering-quality templates with ellipse axial ratios ($=\sqrt{R_f}$) in the range from nearly 1.2 to nearly 5.0. My measurements on such ellipses indicate that the measurements of axial lengths in the range used were normally distributed with a standard deviation of 4%, and not too sensitive to the actual value of the axial ratio. However, the normal distribution of measurements of the orientation of the ellipse long axes had circular standard deviations (σ) strongly dependent on the axial ratio ($\sqrt{R_o}$) of the elliptical marker, approximately according to the formula:

$$2\sigma = \sqrt{(R_o)} \cdot \exp(4.401197 - \sqrt{R_o}).$$

in the range of $\sqrt{R_o}$ indicated above.

(In these tests the markers were ideally elliptical although in nature added errors would arise from unacceptably non-elliptical markers. Siddans (1976) has tackled this practical problem.)

Using these models for the standard deviations of physically measured values, randomly selected simulated 'observational errors' from appropriate normal distributions were automatically applied to the simulated arrays of strained markers to study the effects of the propagation of errors.

All the examples illustrated below show the effects of such simulated observational errors.

DE-STRAINING

The strain ellipse orientation

In a situation of natural deformation there may be many lines of evidence leading to the recognition of the strain ellipse orientation. If, however, we rely solely on the information given by the elliptical markers' shapes and orientations it is more difficult to estimate the strain ellipse direction.

The vector mean of the long axes of the strained particles seems to be the best estimator of the principal extension direction. However, it is not as good as one would like. The modulus of the angular discrepancy, $\bar{v}$, between the true strain ellipse orientation and the vector mean is indicated for four different cases in Fig. 1.

While the discrepancy varies irregularly in magnitude on either side of the true strain ellipse orientation the discrepancies gradually decrease with advancing strain. The angular median (Mardia 1972) shows similar behaviour.

Although the examples in Fig. 1 are severe, it is well to recognise that the difference between the true strain ellipse long axis and the vector mean of as many as 50 elliptical markers' long axes can be as high as 10°.

Clearly, the accuracy of the vector mean is most erratic at low strains. There, fluctuations in $|\bar{v}|$ result from the 'accelerations' of certain critically oriented markers in the array which occur because the particles are changing shape. Some such markers approach the orientation of the strain ellipse's long axis rapidly, overtaking other markers which were initially closer in orientation to the strain ellipse's long axis (see Fig. 2).

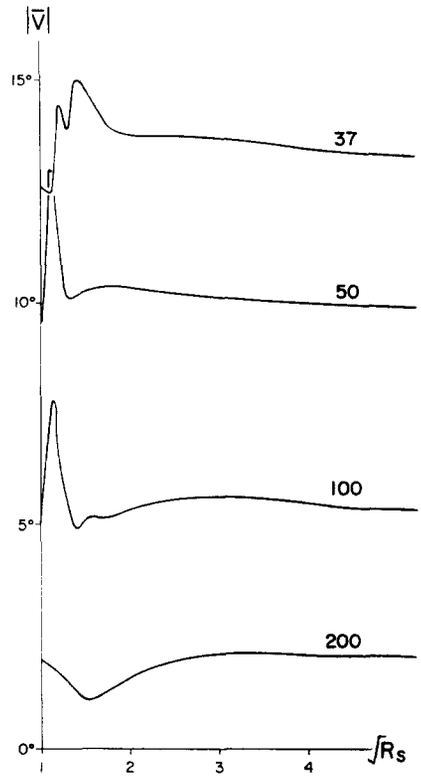

Fig. 1. The change in value of the modulus of the difference in angle between the vector mean of elliptical markers' long axes and the long axis of the strain ellipse with advancing coaxial strain. The numbers of markers in the four samples illustrated are 37, 50, 100 and 200.

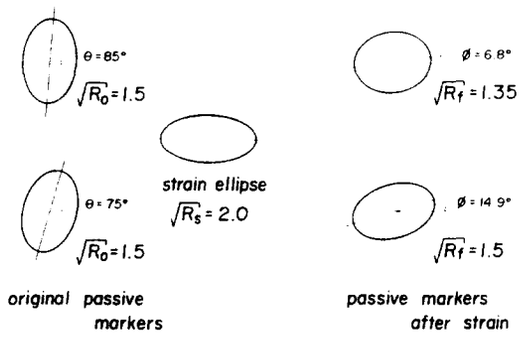

Fig. 2. Elliptical markers at a high angle to the strain ellipse long axis may turn toward the strain ellipse's long axis more quickly than markers which were initially at a lower angle to the strain ellipse. The accelerations of such markers depend on the initial axial ratios ($\sqrt{R_o}$), initial angles (θ) and the strain ellipse ratio ($\sqrt{R_s}$).

The effect of such 'accelerations' of individual markers is most noticeable where it occurs in small samples: there, the few markers which show such behaviour may represent a large proportion of the sample. They can also render it impossible to reconstruct precisely the pre-strain array by any de-straining method which relies solely on the vector mean. It should be noted that an approach using vector magnitudes is also possible (Harvey & Ferguson, 1981).

Comparison of the de-strained array with the pre-strain model

Since we believe the pre-strain array to possess a random fabric we should really make multiple comparisons of the de-strained array with different pre-strain models. This was done in the original application (Borradaile 1976) where the markers under consideration were non-elliptical and, being rigid, did not change shape. In the present context the markers change both orientation and shape and it has been found sufficient to make comparison with a uniform (regular) distribution of orientations for the model of the pre-strain array. (This may be due to the fact that the new shapes of the particles are an dded source of information about the strain.)

Tests for randomness of the de-strained array

Two features of the arrays have been selected as a basis for comparison. In one, the χ^2 method, the strained ('observed') array and the model pre-strain array are compared on the basis of the number of markers occurring in corresponding angular intervals. The test expects at least five counts (markers in our case) to occur in each interval. Furthermore, some statistical texts recommend the use of more than a minimum total number of data (50 counts) and, in others, a minimum number of intervals with a certain number of counts. To maximise the degrees of freedom (ν) of the test, the number of intervals should be kept as high as possible, notwithstanding the other constraints. In my program $\nu > 30$ where there were 200 markers and $\nu \not> 8$ where there were 50 markers.

The match of the de-strained array with the model of the pre-strain array is almost invariably acceptable at the 5% significance level ($\alpha = 0.05$). Only one strain analysis in 1080 failed to successfully de-strain the strained array according to χ^2. The de-straining strain ratio ($\sqrt{R_e}$) which produces a minimum value of χ^2 is the estimate of the true strain ratio $\sqrt{R_s}$.

The second method of testing randomness concerned the length of 'runs' in the de-strained array at each stage in the de-straining process. Runs of a data sequence (e.g. see Davis 1973) are conditions of similarity of adjacent intervals with respect to two alternative, mutually exclusive states. In the present context the de-strained array is divided into equal angular intervals over its range. The number of markers (r) with long axis orientations lying in each interval is compared with the number expected (e) on the basis of a uniform distribution. One state was defined as $r \geqslant e$, the other as $r < e$. Successive intervals representing the same state constitute a run. (As with the χ^2-method care must be taken to take account of the circular nature of the distributions concerned). Where the number of intervals representing each state is >10, the total-number-of-runs in the sequence tends to normal. Then the standard normal variate, z, may be examined to establish the degree to which the de-strained array is random with regard to runs. Just as with the χ^2-minimum method, z^2 may be minimised. The minimum value of z^2 usually occurs at a de-straining ratio which closely matches the true strain ratio, and agrees closely with the χ^2-minimum strain estimate.

The runs-test can only give a strain estimate where there are a large number of strain markers (variable, but usually $\lesssim 50$, to give at least 10 intervals of each state). However, it is sensitive to a different aspect of randomness from χ^2 in the present context. The minimum value of the χ^2-statistic rarely indicates rejection of the hypothesis that the de-strained array is random. In contrast, in the present study the runs-test often rejected the null hypothesis at the same confidence level ($\alpha = 0.05$) where there are less than 35 strain markers. (With 210 different arrays of 75 strain markers the null hypothesis was rejected 16 times).

It appears useful therefore to apply the approaches of the χ^2-minimum and z^2-minimum-for-runs in conjunction. This yields two strain estimates and two tests of the null hypothesis. With small amounts of data, runs-testing may not yield a strain estimate, but tabled values of the critical number of runs are still used to provide an added test of the null hypothesis.

Furthermore, the aspect of randomness with which the runs-test deals may be more relevant to Rf/ϕ analysis under some circumstances. Preferred orientation patterns in pre-strain assemblages of elliptical markers may show clustering and anti-clustering in the angular distribution of their long axes. χ^2 may indicate randomness, yet at the same significance level the hypothesis of randomness can be unacceptable with regard to the number of runs.

Accuracy of the de-straining methods

Results are indicated by the ratio of the estimated strain ellipse $\sqrt{R_e}$ to the actual strain ratio $\sqrt{R_s}$. Our ultimate aim is to achieve $\sqrt{R_e/R_s} = 1$. The graphs (Figs. 3 to 6) give the mean and standard deviation of $\sqrt{R_e/R_s}$ for strain analyses of between 20 and 23 different arrays of simulated field data on deformed elliptical markers.

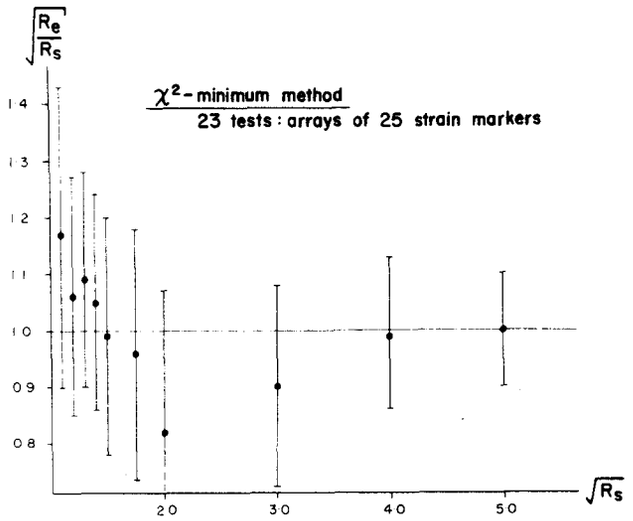

Fig. 3. Results of de-straining using the χ^2-minimum method. Estimates of the strain ellipse axial ratio $\sqrt{R_e}$ for 23 different sets of 25 markers at each of the ten true strain ellipse axial ratios ($\sqrt{R_s}$) are indicated. The estimate $\sqrt{R_e}$ is expressed as a ratio with $\sqrt{R_s}$: $\sqrt{R_e/R_s}$. The mean and standard deviation (error bar) of $\sqrt{R_e/R_s}$ are indicated for the 23 different tests at each strain value.

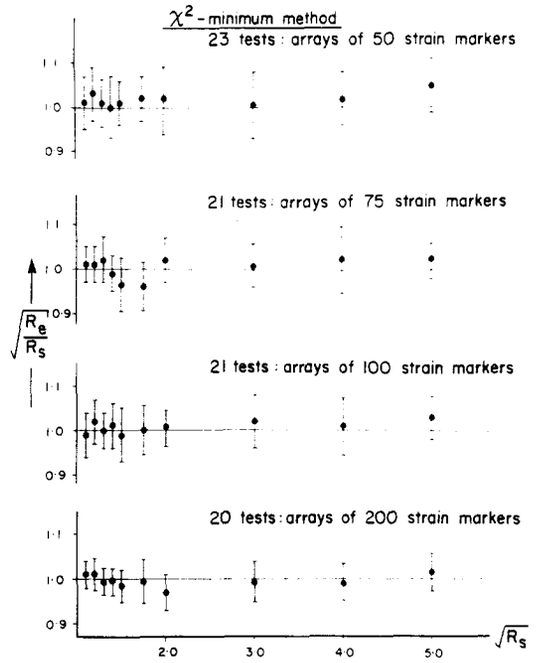

Fig. 4. Results of de-straining by the χ^2-minimum method for larger sample sizes; 50, 75, 100 and 200 markers. The estimated strain ellipse axial ratio $\sqrt{R_e}$ is expressed as a ratio of the true strain ellipse ratio $\sqrt{R_s}$. The mean and standard deviation (error bar) are indicated for 23 tests of different groups of 50 strain markers, for 21 tests of different groups of 75 and 100 strain markers and for 20 tests of different groups of 200 markers.

The χ^2-minimum method gives widely scattered estimates of the strain where there are less than 50 strain markers (Fig. 3). With 50 strain markers the accuracy of the strain estimate is remarkably improved (Fig. 4). The reward of improved accuracy increases slowly as the sample sizes increase from 75 to 200 strain markers.

Runs-testing estimates the strain with lower accuracy (Fig. 5) than the χ^2 method especially with fewer than 75 strain markers. However, the underlying test of randomness of the de-strained array is less easily satisfied with regard to runs. In analyses of natural data, runs-testing may thus draw attention to arrays which cannot be de-strained successfully. Rejection of the hypothesis of randomness occurred many times in the present experiments where there were 50 or 75 strain markers (Fig. 5).

In conclusion, within the premises of this paper, strain analysis by de-straining is improved when more than one aspect of randomness of the de-strained array is considered. The χ^2 and z^2-for-runs methods give two independent strain estimates and two tests of the null hypothesis. With fewer than 50 strain markers, only the χ^2-minimum method yields a strain estimate but both χ^2 and the number-of-runs can be used to test the null hypothesis. With fewer than 75 markers only the χ^2-method gives acceptable accuracy, and accuracy does not appreciably improve with larger samples. The sample size has to be considerably larger to yield comparable accuracy with the z^2-for-runs method. Nevertheless, the number of runs continued to provide an added test for randomness of the de-strained array.

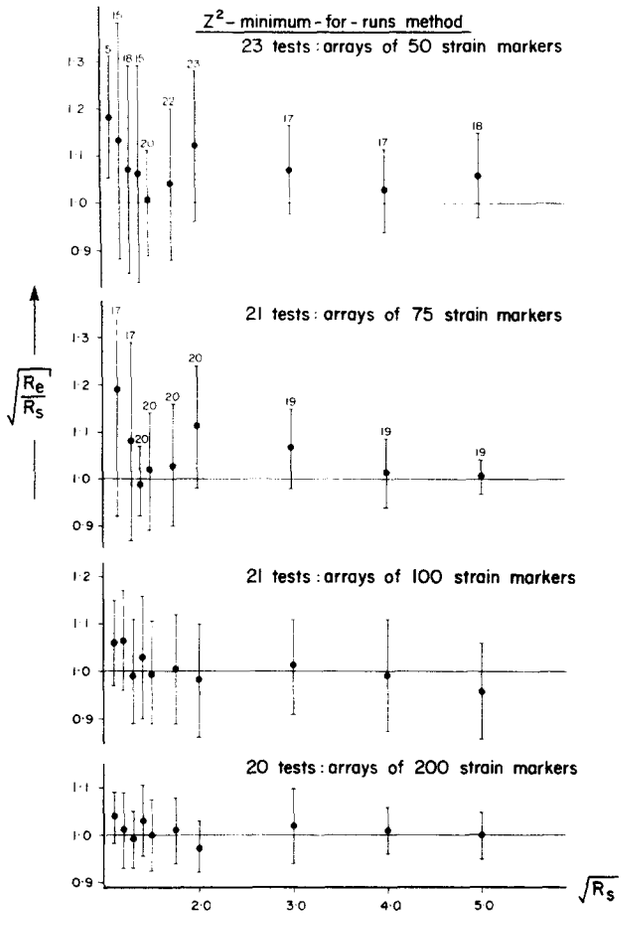

Fig. 5. Results of de-straining by the z^2-minimum-for-runs method. (These results were achieved with exactly the same groups of markers considered in Fig. 4). The ratio of the estimated versus true strain ellipse axial ratio ($\sqrt{R_e/R_s}$) is shown for different true strain ratios ($\sqrt{R_s}$). The man and standard deviation (error bar) are indicated. With 100 markers 21 groups were analysed and with 200 markers 20 groups were tested. With 75 and 50 markers it was often not possible to de-strain the array of markers and successfully minim randomness with regard to the number of runs. The number of groups of data which could be successfully tested is indicated by the number at the end of the error bars in the upper two graphs. Thus with 50 strain markers (top graph), at a true strain ratio of $\sqrt{R_s} = 3.0$, only 17 of the 23 different groups of strained markers could be de-strained successfully.

As a footnote it should be added that with the present assumptions the harmonic mean (Lisle 1976) is invariably as good a strain-estimator where the true strain ellipse ratio $\sqrt{R_s} > 3.0$ (Fig. 6). Strain can be underestimated by the harmonic mean but the bias, which decreases with advancing strain, is towards an overestimate.

Acknowledgements—I thank Don Watson (Lakehead Computer Centre) for provision of facilities, Eric Green and Maurice Benson (Lakehead Mathematics Department) for advice, Richard Lisle for helpful correspondence and Sam Spivak and Wendy Bons for technical support. The research was funded by Natural Sciences and Engineering Research Council of Canada, grant nos. A6861 and E5658.

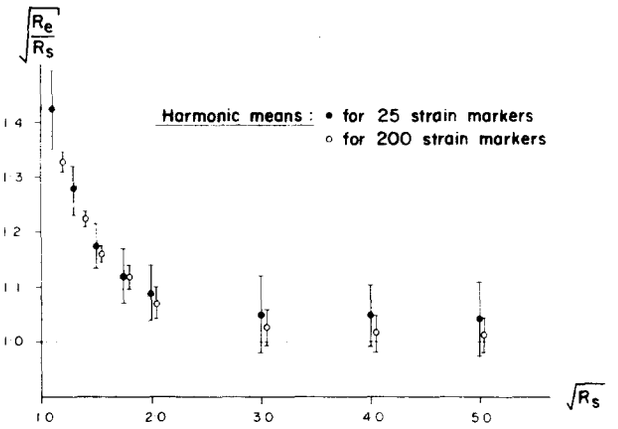

Fig. 6. Harmonic means of the axial ratios of strained elliptical markers may estimate the strain ellipse axial ratio ($\sqrt{R_s}$). The average and standard deviations (error bars) of the ratio of estimated strain to true strain $\sqrt{R_e/R_s}$ are shown for 23 different groups of data with 25 strain markers and 20 different groups of 200 strain markers.

REFERENCES

Borradaile, G. J. 1976. A study of a granite/granite-gneiss transition and accompanying schistosity formation in S.E. Spain. *J. geol. Soc. Lond.* **132**, 417–428.

Davis, J. C. 1973. *Statistics and Data Analysis in Geology*. J. Wiley & Sons, New York.

Dunnet, D. 1969. A technique of finite strain analysis using elliptical particles. *Tectonophysics* **7**, 117–136.

Dunnet, D. & Siddans, A. W. B. 1971. Non-random sedimentary fabrics and their modification by strain. *Tectonophysics* **12**, 307–325.

Elliott, D. 1970. Determination of finite strain and initial shape from deformed elliptical objects. *Bull. geol. Soc. Am.* **81**, 2221–2236.

Harvey, P. K. & Ferguson, C. C. 1981. Directional properties of polygons and their application to finite strain estimation. *Tectonophysics* **74**, T33–T42.

Lisle, R. J. 1977a. Clastic grain shape and orientation in relation to cleavage from the Aberystwyth Grits, Wales. *Tectonophysics* **39**, 381–395.

Lisle, R. J. 1977b. Estimation of the tectonic strain ratio from the mean shape of deformed elliptical markers. *Geol. Mijnb.* **56**, 140–144.

Mardia, K. V. 1972. *Statistics of Directional Data*. Academic Press, London and New York.

Matthews, P. E., Bond, R. A. B. & van der Berg, J. J. 1974. An algebraic method of strain analysis using elliptical markers. *Tectonophysics* **24**, 31–67.

de Paor, D. G. 1980. Some limitations of the Rf/ϕ technique of strain analysis. *Tectonophysics* **64**, T29–T31.

Peach, C. J. & Lisle, R. J. 1979. A Fortran IV program for the analysis of tectonic strain using deformed elliptical markers. *Comput. Geosci.* **5**, 325–334.

Ramsay, J. G. 1967. *Folding and Fracturing of Rocks*. McGraw-Hill, New York.

Seymour, D. B. & Boulter, C. A. 1979. Tests of computerized strain analysis methods by the analysis of simulated deformation of natural unstrained sedimentary fabrics. *Tectonophysics* **58**, 221–235.

Siddans, A. W. B. 1976. Deformed rocks and their textures. *Phil. Trans. R. Soc. Lond.* **A283**, 43–54.

Siddans, A. W. B. 1980a. Elliptical markers and non-coaxial strain increments. *Tectonophysics* **67**, T21–T25.

Siddans, A. W. B. 1980b. Analysis of three-dimensional homogeneous finite strain using ellipsoidal objects. *Tectonophysics* **64**, 1–16.

Shimamoto, R. & Ikeda, Y. 1976. A simple algebraic method for strain estimation from deformed ellipsoidal objects. *Tectonophysics* **36**, 315–317.

le Theoff, B. 1979. Non-coaxial deformation of elliptical particles. *Tectonophysics* **53**, T7–T13.